Discovery of Selective Aminothiazole Aurora Kinase Inhibitors

Carsten B. Andersen[†], Yongqin Wan[†], Jae W. Chang[§], Blake Riggs[¶], Christian Lee[†], Yi Liu[†], Fabio Sessa[‡], Fabrizio Villa[‡], Nicholas Kwiatkowski[§], Melissa Suzuki[‖], Laxman Nallan[†], Rebecca Heald[¶], Andrea Musacchio[‡], and Nathanael S. Gray[§],*

[†]Department of Biological Chemistry, Genomics Institute of the Novartis Research Foundation, 10675 John Jay Hopkins Drive, San Diego, California 92121, [‡]Department of Experimental Oncology, European Institute of Oncology, Via Adamello, 16-20139 Milan, Italy, [§]Department of Cancer Biology, Dana Farber Cancer Institute, Department of Biological Chemistry and Molecular Pharmacology, Harvard Medical School, 250 Longwood Avenue, Boston, Massachusetts 02115, [¶]Department of Molecular and Cell Biology, University of California, Berkeley, California 94720, and [‖]Invitrogen Corporation, Madison, Wisconsin 53558

ABSTRACT Aurora family kinases regulate important events during mitosis including centrosome maturation and separation, mitotic spindle assembly, and chromosome segregation. Misregulation of Aurora kinases due to genetic amplification and protein overexpression results in aneuploidy and may contribute to tumorigenesis. Here we report the discovery of new small molecule aminothiazole inhibitors of Aurora kinases with exceptional kinase selectivity and report a 1.7 Å cocrystal structure with the Aurora B:INCENP complex from *Xenopus laevis*. The compounds recapitulate the hallmarks of Aurora kinase inhibition, including decreased histone H3 serine 10 phosphorylation, failure to complete cytokinesis, and endoreduplication.

*Corresponding author,
nathanael_gray@dfci.harvard.edu.

To maintain fidelity of DNA segregation during cell division, sister chromatids are separated and transported to the cell poles by the mitotic spindle. Errors during this process have the potential to affect genome integrity, which may lead to deregulated growth and tumorigenesis (1). In recent years there has been a focus on understanding the signaling mechanisms involved in the regulation of chromosome separation. It has been established that certain families of protein kinases, such as the Nima-related kinase 2, Polo-like kinase (1), and Aurora kinases (2, 3) are involved in regulating centrosome and spindle function.

Aurora kinases were first discovered in a yeast screen for mutants that displayed improper ploidy following cell division (4). In Drosophila, mutations in Aurora kinase were found to prevent centrosome separation thereby resulting in monopolar spindles (5). There are three known isoforms of Aurora kinase in mammals, Aurora A, B, and C. While Aurora A and B are ubiquitously expressed, Aurora C shows predominant expression in the testis suggesting a possible role in meiosis (6, 7). Although the kinase catalytic domains of all three Aurora isoforms exhibit strong similarity (sequence identity between Aurora B and C to Aurora A is 75% and 72%), the cellular localization, regulation, and substrate specificity of these kinases vary. Aurora A is localized to the centrosome and spindle poles from late S and early G2 through M phase (7). Aurora A binds to and is activated by TPX2 at the G2/M transition, which targets Aurora A to the mitotic spindles (8). Aurora A can phosphorylate histone H3 on serine 10 during centrosome maturation and spindle assembly (9). Aurora B is a chromosome
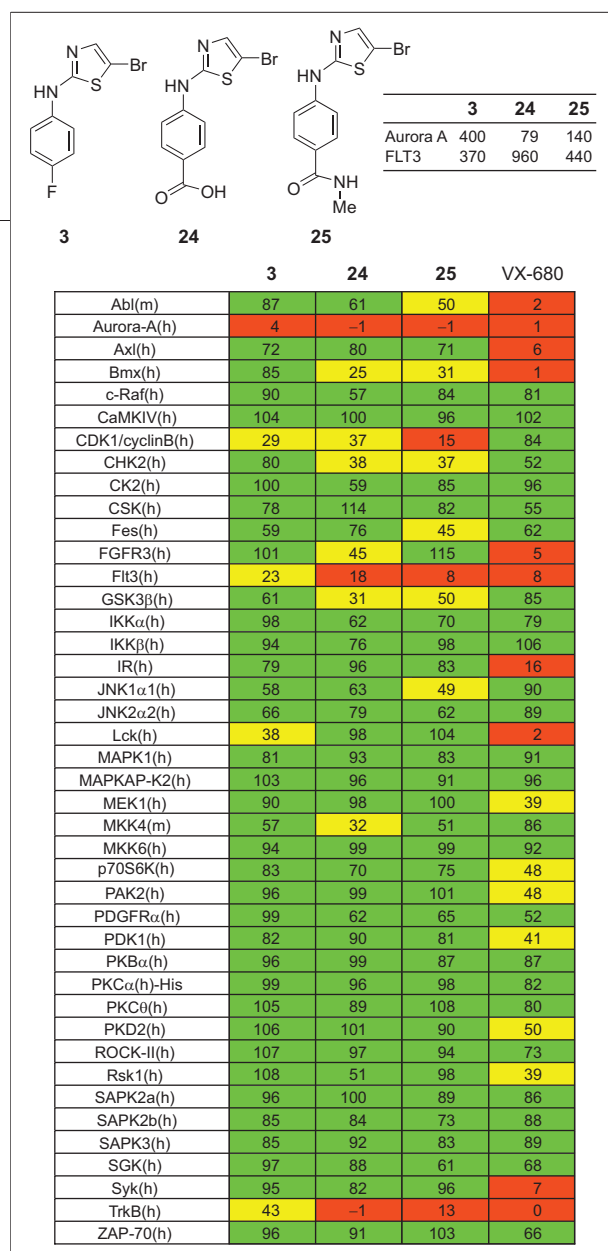
Compound	Aurora A/B/C IC$_{50}$ (nM)
VX-680	0.6 / 18 / 4.6
ZM447439	110 / 130 / nd
Hesperadin	nd / 250 / nd
INH-9d	13 / 79 / 61
INH-1	42 / nd / nd
INH-34	1.4 / <1 / 17
INH-32	1 / nd / nd

VX-680

ZM447439 (X = CH, Y = O, R = H)
INH-13 (X = N, Y = CH$_2$, R = OH)

Hesperadin

INH-9d

INH-1

INH-34

INH-32
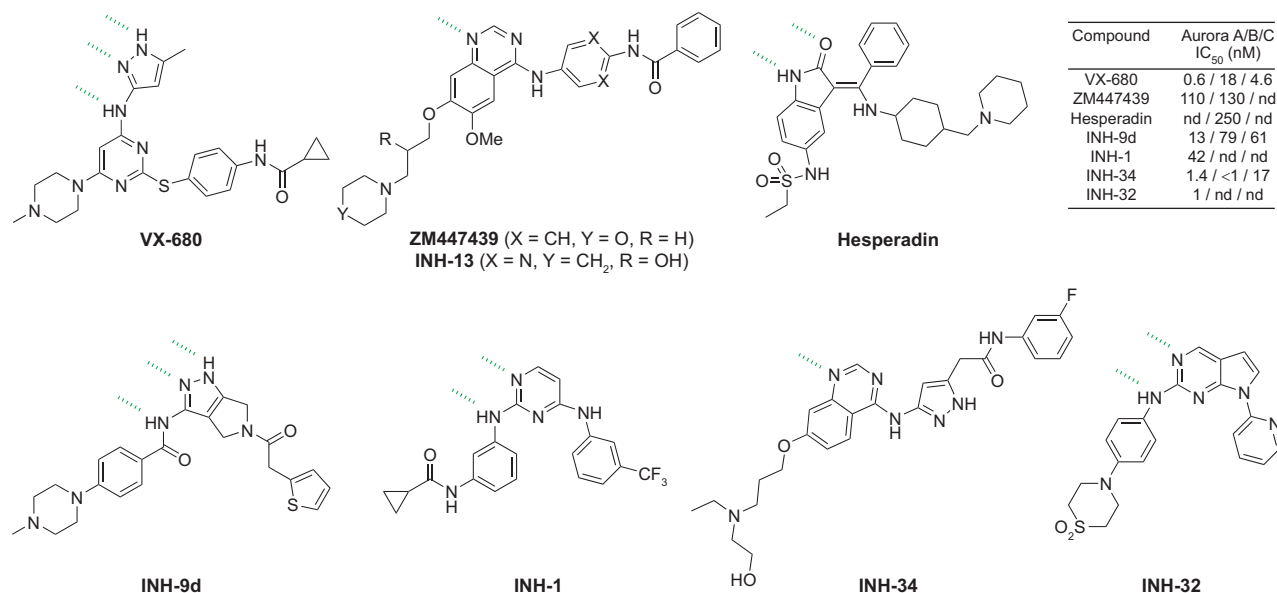
Figure 1. Structure and activity of known inhibitors of Aurora kinase. Structures and names are shown for each compound. The IC$_{50}$ of each compound on Aurora A, B, or C in nanomolar is shown in the table (nd = not determined).

passenger protein that moves from centromeres to the spindle midzone during mitosis. Aurora B is located at the central spindle during late anaphase and at the midbody during telophase and cytokinesis (*10*). The presence of Aurora B at the mitotic spindle appears to be mediated *via* binding to inner centromere protein (INCENP) and survivin (*11*). Like Aurora A, Aurora B can phosphorylate histone H3 on serine 10, but only Aurora B seems necessary for this phosphorylation *in vivo* (*12*). Aurora B is proposed to regulate chromosome condensation and cohesion, bipolar chromosome attachment, the spindle checkpoint and chromosome segregation (*12*). Although less is known about the importance of Aurora C, it can complement some of the functions of Aurora B (*13*).

Aurora A is located at chromosome 20q13 in a region commonly found to be genetically amplified in breast and colon cancer. Both Aurora A and B have the ability to transform cell lines (NIH3T3 or CHO) which are then capable of forming tumors in mice (*14–16*). The roles of the Aurora kinases in cell cycle and tumorigenesis have made them potential targets for the development of small molecule therapeutics. Recently numerous small molecule inhibitors of Aurora kinases have been described - the trisubstituted pyrimidine VX-680

(*17*), the quinazolines ZM447439 and INH-13 (*18*), the indolinone Hesperadin (*19*), the 1,4,5,6-tetrahydro-pyrrolo[3,4-*c*]pyrazole bicycle INH-9d (*20*), the 2,4-diaminopyrimidine INH-1 (*21*), pyrazoloquinazoline INH-34 (*22*), and the pyrrolopyrimidine INH-32 (*23*), in addition to numerous new structures disclosed in the patent literature (Figure 1). The cellular effects of ZM447439 (at 2 μM) and Hesperadin (at 50 nM) appear to mimic those induced by siRNA knockdown of Aurora B including inhibition of serine 10 phosphorylation of histone H3, improper chromosome alignment at metaphase, loss of the spindle checkpoint, and anaphase progression, suggesting that compounds are capable of inhibiting Aurora B in cells. VX-680 inhibits all isoforms of Aurora (A, B, and C) *in vitro* whereas no data are available for the activity of ZM44739 on Aurora C and Hesperadin on Aurora A and C (*17–19*). INH-9d (*20*) is a potent Aurora inhibitor (Aurora A, B, and C enzymatic IC$_{50}$ for A, B, C = 27, 135, 120 nM) that blocks histone H3 phosphorylation at 1 μM and displays antiproliferative effects on various tumor cell lines at concentrations between 50 and 500 nM.

Since one of the main goals in developing Aurora kinase inhibitors is to use them as probes of Aurora function in cellular processes and to investigate their anti-
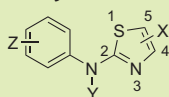
Figure 2. Kinase selectivity profiling of aminothiazoles 3, 24, and 25. Percent activity remaining at 10 μM inhibitor concentration (red <20%, yellow 20–50%, green > 50%). Small table: enzymatic IC$_{50}$ values in nM for Aurora A and Flt3. All kinases are human (h) except Abl and MKK4 which are from mouse (m).

	3	24	25	VX-680
Abl(m)	87	61	50	2
Aurora-A(h)	4	−1	−1	1
Axl(h)	72	80	71	6
Bmx(h)	85	25	31	1
c-Raf(h)	90	57	84	81
CaMKIV(h)	104	100	96	102
CDK1/cyclinB(h)	29	37	15	84
CHK2(h)	80	38	37	52
CK2(h)	100	59	85	96
CSK(h)	78	114	82	55
Fes(h)	59	76	45	62
FGFR3(h)	101	45	115	5
Flt3(h)	23	18	8	8
GSK3β(h)	61	31	50	85
IKKα(h)	98	62	70	79
IKKβ(h)	94	76	98	106
IR(h)	79	96	83	16
JNK1α1(h)	58	63	49	90
JNK2α2(h)	66	79	62	89
Lck(h)	38	98	104	2
MAPK1(h)	81	93	83	91
MAPKAP-K2(h)	103	96	91	96
MEK1(h)	90	98	100	39
MKK4(m)	57	32	51	86
MKK6(h)	94	99	99	92
p70S6K(h)	83	70	75	48
PAK2(h)	96	99	101	48
PDGFRα(h)	99	62	65	52
PDK1(h)	82	90	81	41
PKBα(h)	96	99	87	87
PKCα(h)-His	99	96	98	82
PKCθ(h)	105	89	108	80
PKD2(h)	106	101	90	50
ROCK-II(h)	107	97	94	73
Rsk1(h)	108	51	98	39
SAPK2a(h)	96	100	89	86
SAPK2b(h)	85	84	73	88
SAPK3(h)	85	92	83	89
SGK(h)	97	88	61	68
Syk(h)	95	82	96	7
TrkB(h)	43	−1	13	0
ZAP-70(h)	96	91	103	66

	3	24	25
Aurora A	400	79	140
FLT3	370	960	440

220 nM), and Src (IC$_{50}$ = 350 nM) (18). INH-9d is relatively nonspecific and inhibits a variety of tyrosine kinases including Abl, TrkA, Ret, FGFR1, Lck, and VEGFR2 at concentrations similar to those that inhibit Aurora (20). Collectively, these data indicate that some of the activity of these compounds in cellular experiments and in vivo may result from significant off-target contributions.

RESULTS AND DISCUSSION

In an effort to discover new inhibitors of Aurora A kinase, we screened a library of 4000 kinase-directed heterocycles using a scintillation proximity assay in 384-well format. A His-tagged kinase domain of human Aurora A kinase (residues 107–403) expressed in baculovirus and purified by nickel affinity chromatography was used for the assay (24). Several different scaffolds including 4,6-disubstituted pyrimidines, thiazoles, and pyrazoles emerged as possible leads and were evaluated for their kinase selectivity and for their effects on the cell cycle. We chose to focus our attention on a series of 2-aminophenyl-5-bromothiazoles, such as compound 3, because this class demonstrated the highest degree of kinase selectivity among the available leads, because they were not previously reported as inhibitors of Aurora kinase, and because they possessed a low molecular weight (Figure 2). In order to determine whether the inhibitors were competitive with ATP, we performed kinetic analysis at varied ATP, inhibitor, and substrate concentrations. This analysis demonstrates that aminothiazole analogue 3 acts as a mixed competitive inhibitor versus ATP (Supplemental Figure 1A) and noncompetitive versus substrate (data not shown). Due to the small size of 3 and the observation that it was acting as a mixed competitive inhibitor with respect to ATP, we sought to develop a kinase binding assay that could be used to prove whether the compound were indeed binding in the ATP-binding site. We synthesized a fluorescently labeled derivative in which fluorescein isothiocyanate was coupled through a poly(ethylene glycol) linker to 3 to yield compound 76 (Supplemental Figure 3). Compound 76 possessed an IC$_{50}$ of 1.43 μM for inhibition of Aurora A kinase activity, demonstrating that the activity of the original screening hit 3 was maintained. Binding of compound 76 to Aurora A was competitive with respect to both potent aminothiazole analogues (such as 24 and 27) (Supplemental Figure 1C). Inactive aminothiazole analogues (58) and ATP had little

tumor activity, it would be valuable to have tool compounds that are highly selective kinase inhibitors. Hesperadin is reported to inhibit Mek1, Mapkap-K1, Ampk, Chk1, Phk (phosphorylase kinase), and Lck when tested against a panel of 25 kinases at a concentration of 1 μM (and Cdk1 at slightly higher concentrations) (19). ZM447439 does not show any effects on spindle bipolarity and may not inhibit Aurora A, which is commonly overexpressed in cancer cells. ZM447439 has been reported to inhibit Mek1, Src, and Lck in a limited panel of 16 kinases. VX-680 inhibits a variety of kinases including Flt3 (IC$_{50}$ = 30 nM), Lck (IC$_{50}$ = 80 nM), Itk (IC$_{50}$ =

TABLE 1. IC$_{50}$ against Aurora A in μM for 2-phenylaminothiazoles

Compd no.	5-X	Y	Z	IC$_{50}$, μM	Compd no.	5-X	Y	Z	IC$_{50}$, μM
1	H	H	4-F	>10	28	Br	H	4-CONHCHMeCH$_2$OMe	0.33
2	Cl	H	4-F	1.1	29	Br	H	4-CONMeCH$_2$CH$_2$OMe	0.98
3	Br	H	4-F	0.4	30	Br	H	4-CONHCH$_2$CH$_2$NMe$_2$	5.25
3b	4-Br	H	4-F	>10	31	Br	H	4-CONHCH$_2$CH$_2$NEt$_2$	4.52
4	I	H	4-F	0.5	32	Br	H	4-CONHCH$_2$CH$_2$N⟨morpholine⟩	2.3
5	Br	Me	4-F	>10	33	Br	H	4-CONHCH$_2$CH$_2$N⟨pyrrolidine⟩	5.32
6	Br	H	H	1.1	34	Br	H	3-F	9.3
7	Br	H	4-Cl	3	35	Br	H	3-Me	1.1
8	Br	H	4-Br	2.9	36	Br	H	3-CF$_3$	10
9	Br	H	4-I	>10	37	Br	H	3-OMe	0.9
10	Br	H	4-Me	2.84	38	Br	H	3-SMe	0.5
11	Br	H	4-CF$_3$	2.4	39	Br	H	3-CN	1.5
12	Br	H	4-CN	2.1	40	Br	H	3-CO$_2$Et	2.25
13	Br	H	4-OH	0.51	41	Br	H	3-COOH	0.44
14	Br	H	4-OMe	1.7	42	Br	H	3-CONHCH$_2$CH$_2$OMe	1.22
15	Br	H	4-OCF$_3$	17.2	43	Br	H	3-CONHMe	0.74
16	Br	H	4-OPh	1.4	44	Br	H	2-F	5.5
17	Br	H	4-O⟨pyridine⟩	0.9	45	Br	H	2-Me	3
18	Br	H	4-Ac	1.7	46	Br	H	2-CF$_3$	>10
19	Br	H	4-NO$_2$	13	47	Br	H	2-OMe	2.7
20	Br	H	4-NH$_2$	0.6	48	Br	H	2,4-difluoro	>10
21	Br	H	4-NHCOPh	9.2	49	Br	H	2,5-difluoro	>10
22	Br	H	4-NHAc	0.36	50	Br	H	3,4-dichloro	>10
23	Br	H	4-CO$_2$Et	5.7	51	Br	H	3,5-dichloro	>10
24	Br	H	4-COOH	0.079	52	Br	H	3,5-dimethyl	>10
25	Br	H	4-CONHMe	0.14	53	Br	H	3,5-ditrifluoromethyl	>10
26	Br	H	4-CONHCH$_2$CH$_2$OH	1.48					
27	Br	H	4-CONHCH$_2$CH$_2$OMe	0.097					

or no ability to displace **76** over the concentration range tested. These results suggest that aminothiazole **3** does bind in the same pocket as other ATP competitive Aurora inhibitors but may induce a conformation that exhibits a much lower affinity for ATP.

Synthesis of 5-Halo and 5-Cyanoaminothiazole Analogues. In order to efficiently vary the aniline portion of compound **3** in our investigation of structure–activity relationships, we utilized a two-step synthetic sequence starting from the desired arylthioureas. The

first step involved the formation of the thiazole ring by reaction of arylthiourea with 1,2-dichloro-1-ethoxyethane and the second step consisted of bromination in acetic acid (Supplemental Figure 2). Replacement of the thiazole 5-bromo substituent with chloro or iodo was achieved by reaction of arylthiazol-2-yl-amine with N-chlorosuccinimide or N-iodosuccinimide. Synthesis of 5-cyano analogues was accomplished by amination of 2-chlorothiazole with *tert*-butyldimethylsilyl-protected (6-aminopyridin-3-yl)methanol using sodium hydride, followed by deprotection with HF-pyridine, conversion to the chloride, and nucleophilic displacement with various amines (Supplemental Figure 2). Details for synthesis and compound characterization are described in Methods.

Summary of Structure–Activity Relationships. Over 70 aminothiazole analogues were evaluated in a scintillation proximity assay (SPA) for their ability to inhibit Aurora A kinase activity; the resulting IC_{50} data are listed in Tables 1 and 2. Structure–activity relationships (SARs) for this scaffold as an Aurora kinase inhibitor are summarized in Figure 3. We first investigated analogues in which the 2-(4-fluorophenylamino)-substitutent of the screening hit compound, **3**, was varied. Substitution of the 2-aminophenyl at the para-position resulted in the greatest enhancement in potency against Aurora A and was, interestingly, associated with a wide variety of functionality. Both electron-withdrawing groups, such as fluoro (**1**−**4**), carboxylate (**24**), and carboxyamides (**25**, **27**, **28**), and electron-donating groups, such as hydroxyl (**13**), amino (**20**), and methoxy (**14**), produced marked increases in inhibitory activity against Aurora A. Substitutions at the ortho- and meta-positions of the phenyl ring are less tolerated. In addition to the 2-phenylamino substituted thiazole, thiazoles with benzoylamino (**56**), 2-naphthylamino (**59**), or pyridylamino (**60**−**62**) groups also exhibit single-digit micromolar potency against Aurora kinase; however, a limited exploration of simple amino (**54**), acylamino (**55**), urea (**57**), and alkylamino (**58**) substituents showed diminished activity against Aurora A. N-Methylation of the 2-amino group to yield compound **5** resulted in a loss of activity consistent with formation of a critical hydrogen bond with Ala173 located in the kinase hinge region. When exploring variations at the thiazole 4- and 5- positions, we found that compound **3b**, bearing a bromine at the 4-position instead of 5-position of the aminothiazole, exhibited no activity. Variation of the halogen at the

5-position of the aminothiazole revealed that bromo (**3**) and iodo (**4**) groups have comparable activity (IC_{50} = 500 nM) while the chloro (**2**) derivative is 2-fold less active. A cyano group at 5-position is also tolerated (**63**−**73** in Table 2), with a variety of analogues showing activity in the single-digit micromolar range.
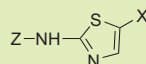
In order to determine how kinase selectivity was altered during the course of the structure–activity optimization, kinase profiling was performed against a panel of 40 different kinases at a concentration of 10 μM (Upstate Biotechnology). The original hit, **3**, displayed a high degree of selectivity for Aurora A kinase with no appreciable inhibition of other kinases at the screening concentration of 10 μM (Figure 2). Aminothiazole **25** inhibited all three Aurora kinases with similar potency when tested using the Z′-LYTE (Invitrogen) assay format at a ATP concentration equal to the apparent K_m (Aurora A IC_{50} = 529 nM, $K_{m,app}$ = 10 μM; Aurora B IC_{50} = 577 nM, $K_{m,app}$ = 64 μM; Aurora C IC_{50} = 758 nM, $K_{m,app}$ = 26 μM). The most potent inhibitors in the current aminothiazole series, **24** and **25**, mostly retained a high degree of selectivity toward Aurora A but also demonstrated some degree of inhibition of Flt3, CDK1/CyclinB, and TrkB. The 50% inhibition values (IC_{50}s) for **3**, **24**, and **25** were 0.37, 0.96, and 0.44 μM for Flt3 and >10 μM, >10 μM, and 4.27 μM for CDK1/cyclinB, respectively (Figure 2). No activity up to a concentration of 10 μM was observed against TrkB in a cellular assay (**25**). It is interesting to note that VX-680 also exhibits cross reactivity between Aurora A and Flt3, suggesting a predilection to a similar inhibitory pharmacophore despite being phylogenetically quite distinct protein kinases.
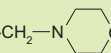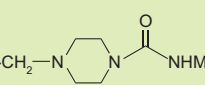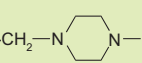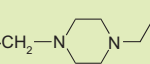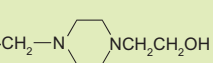
In order to further test the ability of the aminothiazoles to inhibit other kinases, we profiled **25** at a concentration of 1 μM against a panel of 352 diverse kinases using an *in vitro* ATP-site competition binding assay (Supplemental Table 3) (*26*). With this assay, inhibitor **25** only showed binding affinity to Aurora kinases. Comparison of the profile of aminothiazole **25** with clinical Aurora kinase inhibitors such as VX-680 and INH-35 (AZD1152) against the same panel of kinases revealed that **25** is considerably more selective (*27*). The combination of biochemical and *in vitro* binding assays demonstrates that aminothiazoles **24** and **25** are selective Aurora kinase inhibitors and potentially promising scaffolds for further elaboration to obtain more potent inhibitors.

Structure Determination of Aminothiazoles with Aurora Kinase. The high degree of kinase selectivity of the aminothiazoles is unexpected as these small structures possess the requisite hydrogen bond donor and acceptor functionality that could presumably interact with the hinge region of numerous kinases. In order to understand the structural basis for the activity and selectivity of these aminothiazoles, we determined the crystal structure of analogue **25** in the active site of the Aurora B:INCENP complex from *Xenopus laevis* (Xl) (*28*). The amino acid sequences of *Xenopus laevis* and human Aurora A and B are highly homologous to each other (Supplemental Table 1). The crystals contain a tight complex of residues 60–361 of Xl–Aurora B (Aurora B[60–361]) and residues 790–847 of Xl–INCENP (INCENP[790–847]), the so-called IN-box (Figure 4, panel a). The crystallized complex represents an active form of Aurora B (*28*). Crystals were harvested in mother liquor supplemented with 100 μM aminothiazole analogue **25**, incubated for 1 h, and rapidly frozen for X-ray diffraction data collection to a resolution of 1.7 Å (Supplemental Table 2). Electron density "difference" maps with phases calculated from the Aurora B[60–361]: INCENP[790–847] complex revealed additional density in the Aurora B ATP-binding pocket (Figure 4, panel b). The density could be fitted unequivocally with an atomic model of the aminothiazole analogue **25** (Figure 4, panel b). Thus, compound **25** is an ATP-competitive inhibitor of Aurora kinases. It is of note that an identical binding mode was obtained by molecular docking of **3**, the original screening hit, into the published crystal structure of Aurora A (PDB 1mq4) using the docking program GOLD.

The aminothiazole ring of derivative **25** is positioned through stacking interactions with the side chains of Ala120, Leu170 (the "gatekeeper" residue), Ala173, Leu99, and Leu223 (Figure 4, panel b). There are hydrogen bonds with main chain atoms on the hinge loop of Aurora B, and in particular the N3 nitrogen acts as a hydrogen bond acceptor for the amide of Ala173 while the amino group that connects the aminothiazole group with the phenyl moiety is hydrogen bonded to the carbonyl of Ala173 (Figure 4, panel b). The phenyl ring of the 2-anilino substituent makes a complementary stacking interaction with the side chain of Leu99, while the carboxyamide group is largely exposed to solvent apart from the NH donating a proton to the carbonyl of Leu99

TABLE 2. IC$_{50}$ against Aurora A in μM for 2-phenylaminothiazoles

Compd no.	Z	X	IC$_{50}$, μM
54	H	Br	>10
55	COMe	Br	>10
56	COPh	Br	5.5
57	CONHPh	Br	>10
58	CH$_2$CH$_2$Ph	Br	>10
59	1-Nathphyl	Br	5
60	2-Pyridyl	Br	2
61	3-Pyridyl	Br	3.6
62	4-Pyridyl	Br	7.8
63	2-Pyridyl	CN	2.5
69	2-Pyridyl-5-CH$_2$—N(morpholine)	CN	1.4
70	2-Pyridyl-5-CH$_2$—N(piperazine)N-CONHMe	CN	0.88
71	2-Pyridyl-5-CH$_2$—N(piperazine)N—	CN	3.8
72	2-Pyridyl-5-CH$_2$—N(piperazine)N-ethyl	CN	4.4
73	2-Pyridyl-5-CH$_2$—N(piperazine)NCH$_2$CH$_2$OH	CN	5.4

located in the kinase P-loop (Figure 4, panel b). This interaction provides an explanation for the enhanced potency of analogues presenting a hydrogen bond donating group at the aniline 4-position such as an amino (**20**), aminoacetyl (**22**), carboxylate (**24**), and carboxamido (**25** and **27**). The 5-bromo substituent of aminothiazole **25**, is accommodated in a small hydrophobic pocket located adjacent to the gatekeeper residue and is not accessible from the thiazole 4-position, providing an explanation for the lack of activity of compound **3b** (Figure 4, panel b). The size of this hydrophobic pocket differs among kinases due to the highly variable nature of the gate-keeper residue, Leu170,

Figure 3. Summary of SAR for aminothiazole aurora inhibitors. Arrows indicate the position and nature of each substitution tested in a biochemical Aurora A kinase assay.

and may play a role in determining the selectivity of the aminothiazoles. Failure to occupy this hydrophobic pocket (compound **1**) or substitution of a large group at position 5 (data not shown) both render the compounds inactive against Aurora kinase.

Cellular Effects of Aminothiazole Aurora Kinase Inhibitors. In order to investigate the consequences of inhibiting Aurora kinase activity during mitosis, aminothiazole **27** was added to metaphase-arrested cell ex-

tracts prepared from *Xenopus laevis* eggs. These extracts have been extensively used to recapitulate the cell cycle *in vitro* and are ideal for examining perturbations of spindle assembly. Extracts containing sperm chromosomes were cycled to interphase by addition of Ca^{2+}, and aminothiazole **27** was added at a concentration of 10 μM as extracts re-entered mitosis (*29*). Aminothiazole **27** induced a shortening of mitotic spindles relative to the DMSO-treated controls, as well as partial decondensation of the mitotic chromosomes (Figure 5, panels a and b). Similar results were obtained with Hesperadin (data not shown), and our results are consistent with previous studies showing that inhibition or depletion of Aurora B kinase impairs histone H3 phosphorylation and proper chromosome condensation in mitotic cells (*19*). Treatment of extracts with aminothiazole **27** resulted in phenotypes more consistent with depletion of Aurora B kinase than with Aurora A kinase (*30, 31*) and indicate a crucial role for Aurora kinase B activity in maintaining the structure of the mitotic spindle in *Xenopus* egg extracts.

Inhibitors **25** and **27** were next tested for their ability to disrupt the cell cycle. Varying concentrations of compound **25** or **27** were added to HeLa, Colo205, or HCT116 cells for 24 or 48 h, and the cells were subsequently stained with propidium iodide followed by analysis by fluorescent-activated cell sorting (Supplemental Figure 4). After 24 h, aminothiazole analogue **27** produced an accumulation of cells at G2/M with an IC_{50} of 10 μM, whereas the IC_{50} for analogue **25** is closer to 30 μM. This correlates well with potencies of **25** and **27** in the *in vitro* kinase assay (Table 1), with inhibitor **27** exhibiting a lower IC_{50} than **25** in both enzymatic and cellular assays. Inhibition of Aurora B in cells for more than one cell cycle would be expected to lead to duplication of the genome without cytokinesis. Cells do indeed appear to be tetraploid after treatment with 10 μM **25** for 48 h. Although

Figure 4. Interaction of the aminothiazole 25 in the Aurora B ATP-binding pocket. a) Aurora B[60–361] consists of the N-terminal small lobe (gray), a C-terminal helical large lobe (white), and a short C-terminal extension (green). The activation loop (also known as T-loop or activation segment), depicted in red, is important for catalytic activation and substrate recognition. A conserved threonine residue in this loop is phosphorylated as part of the activation mechanism. The αC helix (blue) is also important for the catalytic activity of Aurora B. INCENP[790–847] (orange) crowns the small lobe of Aurora B, stabilizing an active conformation of the kinase (*28*). Aminothiazole 25 shown as ball-and-stick and surrounded by a semitransparent surface, occupies the ATP-binding pocket at the interface between the small and large lobes. b) Ball-and-stick representation of the interaction of the aminothiazole 25 compound with selected residues of Aurora B. Oxygen, nitrogen, sulfur, and bromide atoms are shown in red, blue, orange, and purple, respectively. Carbon atoms in the aminothiazole 25 compound and in Aurora B are white and yellow, respectively. An unbiased $|F_o| - |F_c|$ electron density map (red) contoured at 2.5σ of the aminothiazole 25 compound is shown. Hydrogen bonds are shown as dashed lines.

cells treated with **27** for 48 h do not appear to have undergone a doubling of DNA content, this may indicate that they have already entered apoptosis or that they have arrested in mitosis. Alternatively, the inhibition of CDK1 by **25** which starts to appear at 10 μM *in vitro* (see profiling data Figure 2), may block mitosis and be responsible for the different DNA content of cells after prolonged compound treatment.

Histone H3 is a substrate of Aurora B kinase. To investigate the ability of compound **25** to inhibit the phosphorylation of histone H3, we arrested cells with nocodazole and subjected them to treatment with varying concentrations of **25** for 1 h. Inhibitor **25** reduced histone H3 phosphorylation at Ser10 as assessed by immunostaining with an approximate EC_{50} of 5 μM (Figure 5, panel c). Prolonged treatment with inhibitor **25** (16 h) resulted in many cells becoming multinucleate (Figure 5d). The block of histone H3 phosphorylation (Figure 5, panel c) is in good agreement with cell cycle distribution upon treatment. This further supports to ability of this class of aminothiazoles to act through inhibition of Aurora kinases in cells.

There is a considerable difference between the activity of the compound on Aurora A *in vitro* and in a cellular environment. For example, compound **25** inhibits Aurora A with an enzyme IC_{50} of 140 nM but does not show cellular effects attributable to Aurora inhibition until a concentration of 5–10 μM (cell/enzyme ratio = 35–70). This is in contrast to previously disclosed Aurora inhibitors such as Hesperadin (reported enzyme IC_{50} = 250 nM, cellular block of histone H3 phosphorylation at 50 nM) and VX-680 (reported enzyme IC_{50} = 18 nM, cellular block of histone H3 phosphorylation at 100 nM). Although one possible explanation might be that the significant off-target kinase effects reported with both Hesperadin and VX-680 contribute to their cellular potency, we hypothesized that the more likely explanation is that the aminothiazoles that we have investigated to date lack good cell permeability. This hypothesis is also consistent with the lack of antiproliferative activity on three different cell lines that overexpress Aurora A (AsPC-1, MiaPaca-2, BxPC-3) (data not shown) and that
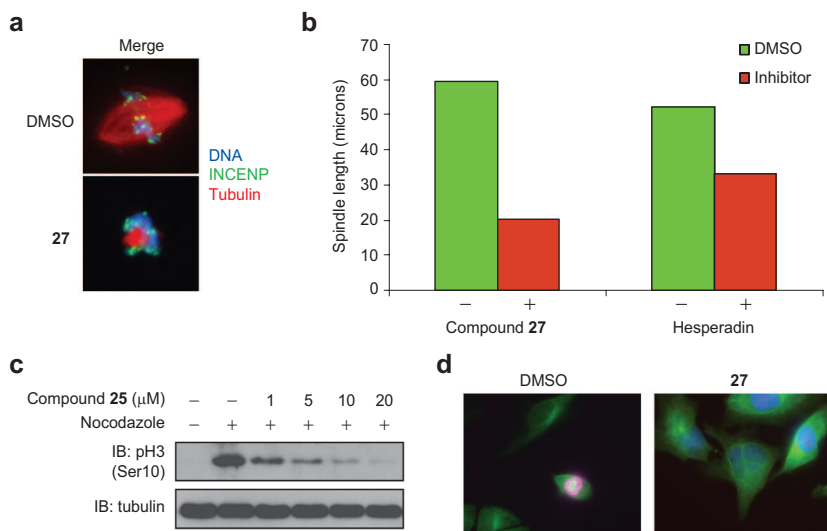
Figure 5. Cellular and *Xenopus* extract results with inhibitors 25 **and** 27. **a)** *Xenopus* **egg extracts treated with DMSO or** 27 **(10 μM) and stained for DNA (blue), INCENP (green), and tubulin (red). b) Spindle length (micrometers) after treatment with DMSO,** 27**, or hesperadin (10 μM). c) Level of histone H3 phosphorylation is determined by SDS-PAGE of total cell extracts and immunostaining performed using antiphospho serine 10 histone H3. HeLa cells first were treated with 100 ng mL^{-1} nocodazole for 20 h prior to treatment with increasing concentration of** 25 **(1, 5, 10, 20 μM) for 3 h. d) HeLa cells treated with DMSO or compound** 27 **for 16 h. Cells were fixed and stained with antiphospho serine 10 histone H3 (red), anti ß-tubulin (green), and DAPI (blue).**

have been shown to exhibit reduced proliferation when treated with siRNAs directed against Aurora A (*32*).

In order to test whether the aminothiazoles exhibit poor cell penetration, we took advantage of the ability of **25** and **27** to inhibit Flt3 kinase activity to make a comparison between enzymatic and cellular potencies against Flt3. To generate a cellular system dependent on Flt3 enzymatic activity, we transformed the murine pre-B cell line with Flt3 and selected for interlukin-3 (IL-3) independent clones (*25, 33*). The dependency of the Flt3–BaF3 cells on Flt3 enzyme activity was verified using the staurosporine-derived inhibitor PKC412 (Flt3 enzyme IC_{50} = 0.01 μM, FLT3–BaF3 IC_{50} = 0.7 μM without IL-3, IC_{50} = 6.7 μM with IL-3). Consistent with the discrepancy between enzymatic and cellular Aurora A activity, both **25** and **27** possessed an antiproliferative IC_{50} of greater than 10 μM against the Flt3 BaF3s which is at least 14-fold greater than the observed enzymatic IC_{50} values of 440 and 730 nM.

**Significance.** A new class of highly selective small molecule inhibitors of Aurora kinases has been discov-
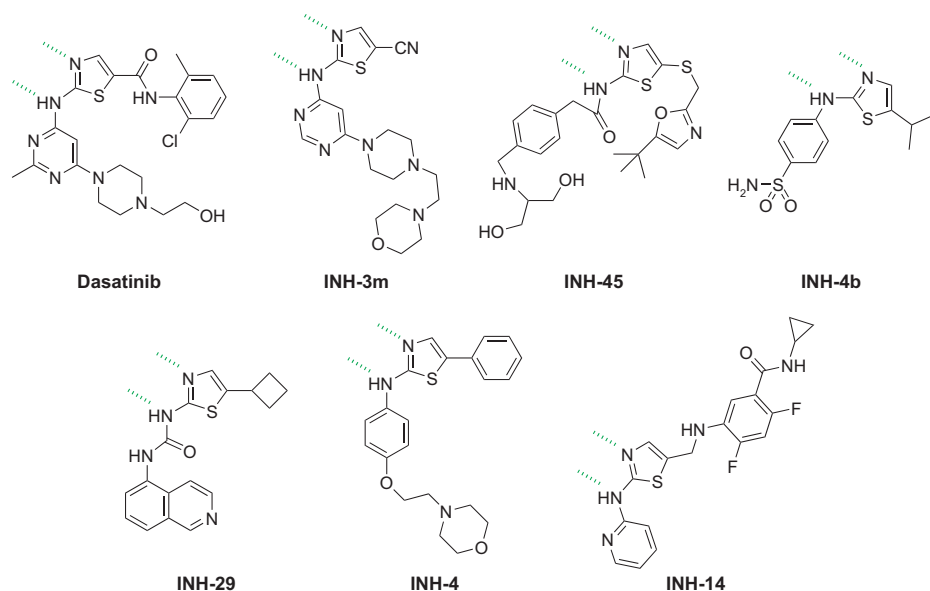
Figure 6. Chemical structures of diverse reported aminothiazole kinase inhibitors.

ered. Aminothiazoles have proven to be versatile scaffolds for building kinase inhibitors targeting several different kinases. These range from nonspecific tyrosine kinase inhibitors such as dasatinib (*34*) and INH-3m (*35*) to compounds of intermediate selectivity such as the pan Cdk inhibitors INH-45 (*36*), INH-4b (*37*), and INH-29 (*38*); to relatively selective inhibitors such as the FLT-3 inhibitor INH-4 (*39*) and the VEGFR-II inhibitor INH-14 (*40*) (Figure 6). Aminothiazoles typically recognize the ATP-binding site by forming a pair of hydrogen bonds to the "hinge" amino acid through the thiazole nitrogen and the 2-NH as observed in the INH-4b Cdk2 cocrystal structure. Although the molecular basis for selectivity of these inhibitors is mostly unknown, there appears be a trend toward broader selectivity from the compounds that strongly exploit the hinge region for potent binding. For example, the two least selective thiazole inhibitors, dasatinib and INH-3m, are capable of forming three-hydrogen bonds through the pyrimidine-aminothiazole motifs. We discovered a simple 5-bromothiazole inhibitor **3** using a biochemical kinase assay and prepared a series of analogues that resulted in the identification of compounds such as **24** and **25** with enzymatic IC_{50} = 79 and 140 nM, respectively, against Aurora A (5-fold improvement relative to **3**). Importantly, the high-degree of kinase selectivity that was observed

for compound **3** was maintained in the more potent analogues **24** and **25**.

We determined the bound conformation of **25** with the Aurora B:INCENP complex isolated from Xl at a resolution of 1.7 Å. The observed conformation demonstrated that the inhibitor binds in the ATP-binding site and forms the expected hydrogen bonds between the aminothiazole and the hinge backbone residues that are observed for most kinase inhibitors (Figure 4, panel b). Selectivity appears to result from the ability of Aurora kinase to accommodate the 5-bromo substituent and to achieve a high degree of hydrophobic complementarity to the phenylamino thiazole pharmacophore. The crystal structures of several chemically distinct classes of Aurora kinase inhibitors have also previously been reported. These structures can be divided into two broad classes depending on the conformation of the activation loop and the region of the ATP-site occupied by the inhibitor (*41*). The first class (type I) recognizes the "active" kinase conformation and binds in the ATP-binding site. This class includes VX-680, Hesperadin, and inhibitor **32**. The second class recognizes a conformation in which the activation loop, including the "DFG" motif, has moved out of the active site to expose an additional hydrophobic binding site adjacent to the ATP-pocket. Inhibitors in this second class (type II) include ZM447439, INH-9d, and INH-34. Unfortunately, ZM447439 is the only type II inhibitor that has been cocrystallized with an activated mutant of Aurora A (T287D, 2c6e), and the activation loop is disordered in this structure. Aminothiazole **25** binds as a type I inhibitor with the thiazole ring occupying a position that appears to be equivalent to that of the pyrrolo-pyrazole core of INH-9d (PHA-680626, 2j4z) and the pyrimidine moiety of the 2,4-disubstituted pyrimidine (2np8) complexed to Aurora kinase (Figure 7). Although a structure of VX-680 with Aurora kinase has not been reported, we note that the methylpyrazole of VX-680 (2f4j) occupies an analogous position when complexed with Abl kinase. The homolo-
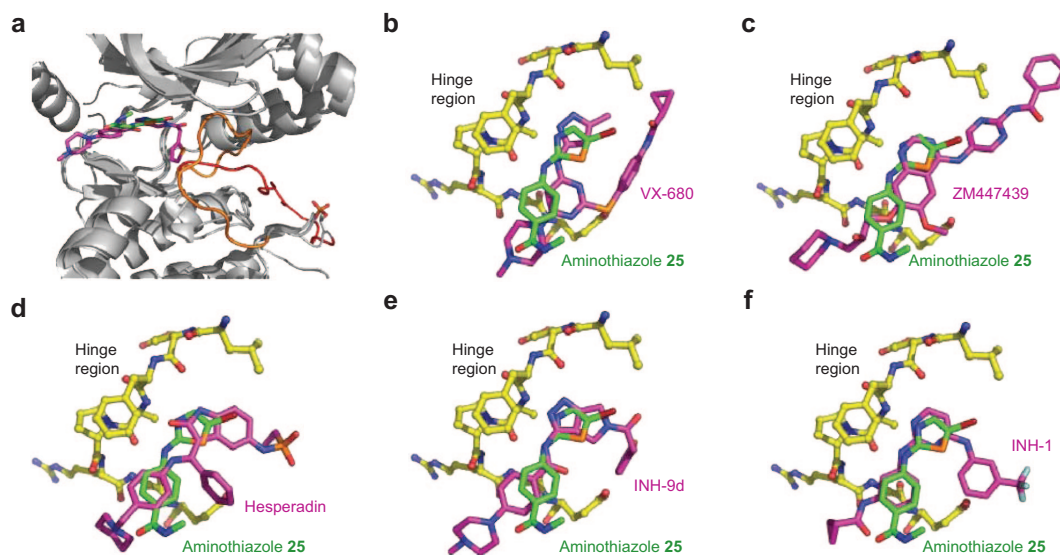
Figure 7. Binding mode of aminothiazole 25 compared to other known Aurora inhibitors. a) Aminothiazole 25 (carbon atoms colored green) bound to Aurora B superimposed with PHA-680626 (carbon atoms colored magenta) bound to Aurora A (PDB code 2j4z) with cartoon representation shown for Aurora A and Aurora B (gray). Highlighted are the phosphorylated T-loop of Aurora B (red) and the nonphosphorylated T-loop of Aurora A (orange). Aminothiazole 25 (carbon atoms colored green) bound to Aurora B with yellow sticks representing Aurora B hinge region superimposed with b) VX-680 (PDB code 2f4j, carbon atoms colored magenta), c) ZM447439 (PDB code 2c6e, carbon atoms colored magenta), d) Hesperadin (PDB code 2bfy, carbon atoms colored magenta), e) PHA-680626 (PDB code 2j4z, carbon atoms colored magenta), and f) 2,4-disubstituted pyrimidine (PDB code 2np8, carbon atoms colored magenta). Chemical structures are shown in Figures 1 and 2. Images created using PyMol.

gous ATP-site interactions formed between the phenylaminothiazole pharmacophore of 25 and the pyrazolopyrimidine moiety of VX-680 may explain the cross reactivity of both compounds with Flt3 in addition to their dominant activity against Aurora kinase. The superposition of these structures provides a wealth of insight into the chemical diversity that can be accommodated within the ATP-cleft of Aurora kinases and provides inspiration for the creation of new "hybrid" compounds (42).

In an effort to study the cellular effects of the aminothiazoles, we demonstrated that the compounds can inhibit histone H3 phosphorylation, block the cell cycle in mitosis, and induce endoreduplication consistent with what has been observed in the literature using siRNAs targeting Aurora A and B. Unfortunately, the aminothiazoles we have investigated to date may have limited utility in some experiments because high micromolar concentrations are required to observe cellular effects. We provide evidence that the lack of cellular potency appears to derive from poor cell penetrability

which may be addressable by further chemical optimization. The most interesting feature of the aminothiazole pharmacophore is that it exhibits exceptional selectivity for Aurora kinases based upon extensive profiling in enzymatic and binding assays. This is in contrast to many reported Aurora inhibitors which exhibit significant cross-reactivity with other kinases. In addition, the low molecular weight of aminothiazole 25 makes it an excellent candidate for further chemical optimization. Therefore the aminothiazoles will be useful mechanistic probes for Aurora-dependent phenomena in cell extract systems. The crystal structure of inhibitor 25 in complex with Aurora B: INCENP can be used in conjunction with other reported cocrystal structures to design new analogues with enhanced potency or selectivity between Aurora isoforms. We expect that optimization of the cellular potency and pharmacological properties of the aminothiazoles could lead to new generation of Aurora inhibitors with sufficient selectivity to be used to elucidate the functions of Aurora-mediated phosphorylations in cellular and *in vivo* models.

METHODS

Synthetic procedures and characterization for all compounds can be found in the Supporting Information.

Kinase Screening and IC$_{50}$ Determination. Kinase activity was performed in 384-well proxiplates using 0.1 μg of kinase per well in kinase buffer (50 mM MOPS pH 7.0, 10 mM MgCl$_2$, 1 mM DTT). Compounds were transferred to each well to a final concentration of 10 μM and kinase buffer containing 1 μM ATP, 10 μCi mL^{-1} ^{33}Pγ-ATP. For IC$_{50}$ determination the final concentration of 10 μM ATP was used. Plates were incubated 1 h at RT before terminating the reaction with 1 M ATP, 1 mM EDTA, 50 mg mL^{-1} SPA beads (Amersham/pharmacia/GE health) and counted on topcount. Compounds with more than 50% inhibition of kinase activity were retested to determine IC$_{50}$. Kinase selectivity was determined by profiling leads on 40 different kinases (kinaseprofiler, Upstate). Z′-LYTE Enzymatic Kinase Assay format (Invitrogen Corp., Carlsbad, CA) in the SelectScreen Kinase Profiling Service (Invitrogen Discovery Sciences, Madison, WI). Compounds were assayed at a starting concentration of 30 μM, and $K_{m\ [app]}$ ATP, following the detailed procedures described in the SelectScreen. Customer Protocol and Assay Conditions document located at www.invitrogen.com/kinase profiling.

Histone H3 Ser10 Phosphorylation. Fifty thousand HeLa cells plated in 12-well plates were treated with 100 ng mL^{-1} nocodazole for 20 h prior to 1 h incubation with compound. Cells were lysed in 2× sample buffer. Samples of total cell extracts, equal to one-third of the cells per well, were subjected to SDS-PAGE and Western blotting with anti-phospho-serine 10 histone H3 (Cell Signaling) to determine phosphorylation state.

Fluorescence-Activated Cell Sorting Analysis. HeLa cells were treated with compound for various periods of time. Cells were trypsinized, washed once in PBS, and fixed for 20 min at −20 °C. Cells were resuspended in PBS, 1 mM EDTA, 100 μg mL^{-1} RNase and incubated for 30 min at 37 °C, prior to addition of 10 μg mL^{-1} final concentration of propidium iodide (PI). Cell cycle distribution was determined on Beckman FACScalibur (BD Biosciences) and analyzed on FlowJo (Treestar).

High Throughput Microscopy (HTM). Alternatively cell cycle distribution was quantified using a confocal microscope system with capable of imaging a 384-well plate as follows. Four thousand HeLa cells were plated in each well of a 384-well plate, 24 h later varying concentrations of compounds were added at various times and plates were fixed in 4% paraformaldehyde and stained with 4′,6-diamidino-2-phenylindole (DAPI). Automated acquisition of image from each well was performed and analyzed on an EIDAQ 100 high throughput microscope (Q3DM/Beckman Coulter).

Cell Proliferation Assay. Cells were plated in 96-well plates and subjected to serial dilutions of compound. Forty eight hours later cell viability was measured using CellTiter96 (Promega) following the manufacturer's protocol.

Microscopy. Hela cells were plated on coverslips and subjected to various compound treatments 20 h later. Compound treatments were terminated by washing the coverslips twice with PBS and fixing them in 4% paraformaldehyde at 37 °C for 10 min. The coverslips were washed in PBS and subsequently incubated in blocking solution (PBS 0.1% Triton X-100 and 5% BSA) for a minimum of 1 h. Coverslips were stained for 1 h with 1:300 anti-phospho-serine 10 histone H3 in blocking solution, 5% BSA, followed by incubation for 1 h 1:1000 anti-rabbit Cy3 in blocking solution. In some cases coverslips were also stained with FITC labeled anti-B-tubulin in blocking solution.

Crystallization and Structure Determination. The conditions for expression, purification, and structure determination of Aurora B$^{60-361}$:INCENP$^{790-847}$ have been previously described (28). Crystals obtained by microseeding were gradually transferred in cryo-buffer (19% PEG400, 100 mM Bis-Tris-Propane pH 6.5, 2 mM TCEP), and then incubated with 1/100 (vol/vol) of a 10 mM solution of analogue **25** dissolved in DMSO. After a 1 h incubation with the inhibitor, crystals were flash-frozen. X-ray diffraction data from single crystals were collected at beamline ID14-1 at the European Synchroton Radiation Facility (Grenoble, France). Data processing was carried out with DENZO/SCALEPACK (43). For subsequent calculations, we used the CCP4 suite (44). Molecular replacement was carried out with MOLREP (45) using the Aurora-B coordinates as search model (PDB ID code 2bfx). Iterative model building was carried out with Coot (46) and Refmac (47) resulting in a good model (Supplemental Table 1).

Xenopus Extracts. A solution of compound **27** in water/DMSO (75%/25% by volume) at a concentration of 100 μM was prepared. This stock solution was used to deliver compound to the extracts at a final concentration of 10 μM. All controls were performed with equal volumes of 25% DMSO solvent. _Xenopus laevis_ extracts were prepared according to Hannak and Heald (29). Cytostatic factor (CSF)-arrested extracts were cycled into interphase by addition of a calcium solution (4 mM CaCl$_2$, 100 mM KCl, and 1 mM MgCl$_2$) and assayed for the presence of intact interphase nuclei after a 1 h incubation. Control solvent or compound **27** was added to the interphase extracts, and entry into mitosis was initiated by adding an equal volume of CSF-arrested extract. Spindle formation occurred within 30 min and was visualized by addition of 0.1 μg mL^{-1} rhodamine-labeled tubulin. Reactions were spun onto coverslips and fixed as previously described (48). Immunostaining was performed using α-INCENP antibody at 1:5000 (ABcam). Images were collected using an Olympus fluorescence microscope (model BX51) with a dry 40× objective, a cooled CCD camera (model Orcall, Hamamatsu), and MetaMorph software (Molecular Devices), also used for spindle measurements. Error bars indicate the standard deviation; sample size for control and compound treated spindles is $n = 33$.

REFERENCES

1. Nigg, E. A. (2002) Centrosome aberrations: cause or consequence of cancer progression? _Nat. Rev. Cancer 2_, 815–825.
2. Glover, D. M. (2005) Polo kinase and progression through M phase in Drosophila: a perspective from the spindle poles, _Oncogene 24_, 230–237.
3. O'Connell, M. J., Krien, M. J., and Hunter, T. (2003) Never say never. The NIMA-related protein kinases in mitotic control, _Trends Cell Biol. 13_, 221–228.

4. Chan, C. S., and Botstein, D. (1993) Isolation and characterization of chromosome-gain and increase-in-ploidy mutants in yeast, *Genetics 135*, 677–691.

5. Glover, D. M., Leibowitz, M. H., McLean, D. A., and Parry, H. (1995) Mutations in aurora prevent centrosome separation leading to the formation of monopolar spindles, *Cell 81*, 95–105.

6. Tseng, T. C., Chen, S. H., Hsu, Y. P., and Tang, T. K. (1998) Protein kinase profile of sperm and eggs: cloning and characterization of two novel testis-specific protein kinases (AIE1, AIE2) related to yeast and fly chromosome segregation regulators, *DNA Cell Biol. 17*, 823–833.

7. Kimura, M., Kotani, S., Hattori, T., Sumi, N., Yoshioka, T., Todokoro, K., and Okano, Y. (1997) Cell cycle-dependent expression and spindle pole localization of a novel human protein kinase, Aik, related to Aurora of Drosophila and yeast Ipl1, *J. Biol. Chem. 272*, 13766–13771.

8. Kufer, T. A., Sillje, H. H., Korner, R., Gruss, O. J., Meraldi, P., and Nigg, E. A. (2002) Human TPX2 is required for targeting Aurora-A kinase to the spindle, *J. Cell Biol. 158*, 617–623.

9. Dutertre, S., Descamps, S., and Prigent, C. (2002) On the role of aurora-A in centrosome function, *Oncogene 21*, 6175–6183.

10. Terada, Y., Tatsuka, M., Suzuki, F., Yasuda, Y., Fujita, S., and Otsu, M. (1998) AIM-1: a mammalian midbody-associated protein required for cytokinesis, *EMBO J. 17*, 667–676.

11. Shannon, K. B., and Salmon, E. D. (2002) Chromosome dynamics: new light on Aurora B kinase function, *Curr. Biol. 12*, R458–R460.

12. Giet, R., McLean, D., Descamps, S., Lee, M. J., Raff, J. W., Prigent, C., and Glover, D. M. (2002) Drosophila Aurora A kinase is required to localize D-TACC to centrosomes and to regulate astral microtubules, *J. Cell Biol. 156*, 437–451.

13. Sasai, K., Katayama, H., Stenoien, D. L., Fujii, S., Honda, R., Kimura, M., Okano, Y., Tatsuka, M., Suzuki, F., Nigg, E. A., Earnshaw, W. C., Brinkley, W. R., and Sen, S. (2004) Aurora-C kinase is a novel chromosomal passenger protein that can complement Aurora-B kinase function in mitotic cells, *Cell Motil. Cytoskeleton 59*, 249–263.

14. Bischoff, J. R., Anderson, L., Zhu, Y., Mossie, K., Ng, L., Souza, B., Schryver, B., Flanagan, P., Clairvoyant, F., Ginther, C., Chan, C. S., Novotny, M., Slamon, D. J., and Plowman, G. D. (1998) A homologue of Drosophila aurora kinase is oncogenic and amplified in human colorectal cancers, *EMBO J. 17*, 3052–3065.

15. Zhou, H., Kuang, J., Zhong, L., Kuo, W. L., Gray, J. W., Sahin, A., Brinkley, B. R., and Sen, S. (1998) Tumour amplified kinase STK15/BTAK induces centrosome amplification, aneuploidy and transformation, *Nat. Genet. 20*, 189–193.

16. Ota, T., Suto, S., Katayama, H., Han, Z. B., Suzuki, F., Maeda, M., Tanino, M., Terada, Y., and Tatsuka, M. (2002) Increased mitotic phosphorylation of histone H3 attributable to AIM-1/Aurora-B overexpression contributes to chromosome number instability, *Cancer Res. 62*, 5168–5177.

17. Harrington, E. A., Bebbington, D., Moore, J., Rasmussen, R. K., Ajose-Adeogun, A. O., Nakayama, T., Graham, J. A., Demur, C., Hercend, T., Diu-Hercend, A., Su, M., Golec, J. M., and Miller, K. M. (2004) VX-680, a potent and selective small-molecule inhibitor of the Aurora kinases, suppresses tumor growth in vivo, *Nat Med 10*, 262–7.

18. Ditchfield, C., Johnson, V. L., Tighe, A., Ellston, R., Haworth, C., Johnson, T., Mortlock, A., Keen, N., and Taylor, S. S. (2003) Aurora B couples chromosome alignment with anaphase by targeting BubR1, Mad2, and Cenp-E to kinetochores, *J. Cell Biol. 161*, 267–280.

19. Hauf, S., Cole, R. W., LaTerra, S., Zimmer, C., Schnapp, G., Walter, R., Heckel, A., van Meel, J., Rieder, C. L., and Peters, J. M. (2003) The small molecule Hesperadin reveals a role for Aurora B in correcting kinetochore-microtubule attachment and in maintaining the spindle assembly checkpoint, *J. Cell Biol. 161*, 281–294.

20. Fancelli, D., Berta, D., Bindi, S., Cameron, A., Cappella, P., Carpinelli, P., Catana, C., Forte, B., Giordano, P., Giorgini, M. L., Mantegani, S., Marsiglio, A., Meroni, M., Moll, J., Pittala, V., Roletto, F., Severino, D., Soncini, C., Storici, P., Tonani, R., Varasi, M., Vulpetti, A., and Vianello, P. (2005) Potent and selective Aurora inhibitors identified by the expansion of a novel scaffold for protein kinase inhibition, *J. Med. Chem. 48*, 3080–3084.

21. Tari, L. W., Hoffman, I. D., Bensen, D. C., Hunter, M. J., Nix, J., Nelson, K. J., McRee, D. E., and Swanson, R. V. (2007) Structural basis for the inhibition of Aurora A kinase by a novel class of high affinity disubstituted pyrimidine inhibitors, *Bioorg. Med. Chem. Lett. 17*, 688–691.

22. Mortlock, A. A., Foote, K. M., Heron, N. M., Jung, F. H., Pasquet, G., Lohmann, J. J., Warin, N., Renaud, F., De Savi, C., Roberts, N. J., Johnson, T., Dousson, C. B., Hill, G. B., Perkins, D., Hatter, G., Wilkinson, R. W., Wedge, S. R., Heaton, S. P., Odedra, R., Keen, N. J., Crafter, C., Brown, E., Thompson, K., Brightwell, S., Khatri, L., Brady, M. C., Kearney, S., McKillop, D., Rhead, S., Parry, T., and Green, S. (2007) Discovery, synthesis, and in vivo activity of a new class of pyrazoloquinazolines as selective inhibitors of aurora B kinase, *J. Med. Chem. 50*, 2213–2224.

23. Moriarty, K. J., Koblish, H. K., Garrabrant, T., Maisuria, J., Khalil, E., Ali, F., Petrounia, I. P., Crysler, C. S., Maroney, A. C., Johnson, D. L., and Galemmo, R. A., Jr (2006) The synthesis and SAR of 2-amino-pyrrolo[2, 3-d]pyrimidines: a new class of Aurora-A kinase inhibitors, *Bioorg. Med. Chem. Lett. 16*, 5778–5783.

24. Cheetham, G. M., Knegtel, R. M., Coll, J. T., Renwick, S. B., Swenson, L., Weber, P., Lippke, J. A., and Austen, D. A. (2002) Crystal structure of aurora-2, an oncogenic serine/threonine kinase, *J. Biol. Chem. 277*, 42419–42422.

25. Melnick, J. S., Janes, J., Kim, S., Chang, J. Y., Sipes, D. G., Gunderson, D., Jarnes, L., Matzen, J. T., Garcia, M. E., Hood, T. L., Beigi, R., Xia, G., Harig, R. A., Asatryan, H., Yan, S. F., Zhou, Y., Gu, X. J., Saadat, A., Zhou, V., King, F. J., Shaw, C. M., Su, A. I., Downs, R., Gray, N. S., Schultz, P. G., Warmuth, M., and Caldwell, J. S. (2006) An efficient rapid system for profiling the cellular activities of molecular libraries, *Proc. Natl. Acad. Sci. U.S.A. 103*, 3153–3158.

26. Fabian, M. A., Biggs, W. H., 3rd, Treiber, D. K., Atteridge, C. E., Azimioara, M. D., Benedetti, M. G., Carter, T. A., Ciceri, P., Edeen, P. T., Floyd, M., Ford, J. M., Galvin, M., Gerlach, J. L., Grotzfeld, R. M., Herrgard, S., Insko, D. E., Insko, M. A., Lai, A. G., Lelias, J. M., Mehta, S. A., Milanov, Z. V., Velasco, A. M., Wodicka, L. M., Patel, H. K., Zarrinkar, P. P., and Lockhart, D. J. (2005) A small molecule-kinase interaction map for clinical kinase inhibitors, *Nat. Biotechnol. 23*, 329–336.

27. Karaman, M. W., Herrgard, S., Treiber, D. K., Gallant, P., Atteridge, C. E., Campbell, B. T., Chan, K. W., Ciceri, P., Davis, M. I., Edeen, P. T., Faraoni, R., Floyd, M., Hunt, J. P., Lockhart, D. J., Milanov, Z. V., Morrison, M. J., Pallares, G., Patel, H. K., Pritchard, S., Wodicka, L. M., and Zarrinkar, P. P. (2008) A quantitative analysis of kinase inhibitor selectivity, *Nat. Biotechnol. 26*, 127–132.

28. Sessa, F., Mapelli, M., Ciferri, C., Tarricone, C., Areces, L. B., Schneider, T. R., Stukenberg, P. T., and Musacchio, A. (2005) Mechanism of Aurora B activation by INCENP and inhibition by hesperadin, *Mol. Cell 18*, 379–391.

29. Hannak, E., and Heald, R. (2006) Investigating mitotic spindle assembly and function in vitro using Xenopus laevis egg extracts, *Nat. Protoc. 1*, 2305–2314.

30. Gadea, B. B., and Ruderman, J. V. (2006) Aurora B is required for mitotic chromatin-induced phosphorylation of Op18/Stathmin, *Proc. Natl. Acad. Sci. U.S.A. 103*, 4493–4498.

31. Liu, Q., and Ruderman, J. V. (2006) Aurora A, mitotic entry, and spindle bipolarity, *Proc. Natl. Acad. Sci. U.S.A. 103*, 5811–5816.

32. Warner, S. L., Bearss, D. J., Han, H., and Von Hoff, D. D. (2003) Targeting Aurora-2 kinase in cancer, *Mol. Cancer Ther. 2*, 589–595.

33. Weisberg, E., Boulton, C., Kelly, L. M., Manley, P., Fabbro, D., Meyer, T., Gilliland, D. G., and Griffin, J. D. (2002) Inhibition of mutant FLT3 receptors in leukemia cells by the small molecule tyrosine kinase inhibitor PKC412, *Cancer Cell 1*, 433–443.

34. Lombardo, L. J., Lee, F. Y., Chen, P., Norris, D., Barrish, J. C., Behnia, K., Castaneda, S., Cornelius, L. A., Das, J., Doweyko, A. M., Fairchild, C., Hunt, J. T., Inigo, I., Johnston, K., Kamath, A., Kan, D., Klei, H., Marathe, P., Pang, S., Peterson, R., Pitt, S., Schieven, G. L., Schmidt, R. J., Tokarski, J., Wen, M. L., Wityak, J., and Borzilleri, R. M. (2004) Discovery of N-(2-chloro-6-methyl- phenyl)-2-(6-(4-(2-hydroxyethyl)- piperazin-1-yl)-2-methylpyrimidin-4- ylamino)-thiazole-5-carboxamide (BMS-354825), a dual Src/Abl kinase inhibitor with potent antitumor activity in preclinical assays, *J. Med. Chem. 47*, 6658–6661.

35. Sisko, J. T., Tucker, T. J., Bilodeau, M. T., Buser, C. A., Ciecko, P. A., Coll, K. E., Fernandes, C., Gibbs, J. B., Koester, T. J., Kohl, N., Lynch, J. J., Mao, X., McLoughlin, D., Miller-Stein, C. M., Rodman, L. D., Rickert, K. W., Sepp-Lorenzino, L., Shipman, J. M., Thomas, K. A., Wong, B. K., and Hartman, G. D. (2006) Potent 2-[(pyrimidin-4-yl)amine}−1, 3-thiazole-5 carbonitrile-based inhibitors of VEGFR-2 (KDR) kinase, *Bioorg. Med. Chem. Lett. 16*, 1146–1150.

36. Kim, K. S., Kimball, S. D., Misra, R. N., Rawlins, D. B., Hunt, J. T., Xiao, H. Y., Lu, S., Qian, L., Han, W. C., Shan, W., Mitt, T., Cai, Z. W., Poss, M. A., Zhu, H., Sack, J. S., Tokarski, J. S., Chang, C. Y., Pavletich, N., Kamath, A., Humphreys, W. G., Marathe, P., Bursuker, I., Kellar, K. A., Roongta, U., Batorsky, R., Mulheron, J. G., Bol, D., Fairchild, C. R., Lee, F. Y., and Webster, K. R. (2002) Discovery of aminothiazole inhibitors of cyclin-dependent kinase 2: synthesis, X-ray crystallographic analysis, and biological activities, *J. Med. Chem. 45*, 3905–3927.

37. Vulpetti, A., Casale, E., Roletto, F., Amici, R., Villa, M., and Pevarello, P. (2006) Structure-based drug design to the discovery of new 2-aminothiazole CDK2 inhibitors, *J. Mol. Graphics Modell. 24*, 341–348.

38. Helal, C. J., Sanner, M. A., Cooper, C. B., Gant, T., Adam, M., Lucas, J. C., Kang, Z., Kupchinsky, S., Ahlijanian, M. K., Tate, B., Menniti, F. S., Kelly, K., and Peterson, M. (2004) Discovery and SAR of 2-aminothiazole inhibitors of cyclin-dependent kinase 5/p25 as a potential treatment for Alzheimer's disease, *Bioorg. Med. Chem. Lett. 14*, 5521–5525.

39. Furet, P., Bold, G., Meyer, T., Roesel, J., and Guagnano, V. (2006) Aromatic interactions with phenylalanine 691 and cysteine 828: a concept for FMS-like tyrosine kinase-3 inhibition. Application to the discovery of a new class of potential antileukemia agents, *J. Med. Chem. 49*, 4451–4454.

40. Borzilleri, R. M., Bhide, R. S., Barrish, J. C., D'Arienzo, C. J., Derbin, G. M., Fargnoli, J., Hunt, J. T., Jeyaseelan, R., Sr., Kamath, A., Kukral, D. W., Marathe, P., Mortillo, S., Qian, L., Tokarski, J. S., Wautlet, B. S., Zheng, X., and Lombardo, L. J. (2006) Discovery and evaluation of N-cyclopropyl- 2, 4-difluoro-5((2-(pyridin-2-ylamino)thiazol-5- ylmethyl)amino)benzamide (BMS-605541), a selective and orally efficacious inhibitor of vascular endothelial growth factor receptor-2, *J. Med. Chem. 49*, 3766–3769.

41. Liu, Y., and Gray, N. S. (2006) Rational design of inhibitors that bind to inactive kinase conformations, *Nat. Chem. Biol. 2*, 358–364.

42. Okram, B., Nagle, A., Adrian, F. J., Lee, C., Ren, P., Wang, X., Sim, T., Xie, Y., Wang, X., Xia, G., Spraggon, G., Warmuth, M., Liu, Y., and Gray, N. S. (2006) A general strategy for creating "inactive-conformation" abl inhibitors, *Chem. Biol. 13*, 779–786.

43. Otwinowski, Z., and Minor, W (1997) Processing of X-ray diffraction data collected in oscillation mode, *Methods Enzymol. 276*, 307–326.

44. Collaborative Computational Project Number 4. (1994) The CCP4 suite: programs for protein crystallography, *Acta Crystallogr., Sect. D: Biol. Crystallogr. 50*, 760–763.

45. Vagin, A., and Teplyakov, A. (1997) MOLREP: an automated program for molecular replacement, *J. Appl. Crystallogr. 30*, 1022–1025.

46. Emsley, P., and Cowtan, K. (2004) Coot: model-building tools for molecular graphics, *Acta Crystallogr., Sect. D: Biol. Crystallogr. 60*, 2126–2132.

47. Murshudov, G. N., Vagin, A. A., and Dodson, E. J. (1997) Refinement of macromolecular structures by the maximum-likelihood method, *Acta Crystallogr., Sect. D: Biol. Crystallogr. 53*, 240–255.

48. Wignall, S. M., and Heald, R. (2001) Methods for the study of centrosome-independent spindle assembly in Xenopus extracts, *Methods Cell Biol. 67*, 241–256.